NREL/TP-411-5013 • UC Category: 270,233 • DE92016430

Photovoltaic Advanced Research and Development Project: Solar Radiation Research Annual Report

1 October 1990 – 30 September 1991

R. Hulstrom, T. Cannon, T. Stoffel, and C. Riordan

National Renewable Energy Laboratory
1617 Cole Boulevard
Golden, Colorado 80401-3393
Operated by Midwest Research Institute
for the U.S. Department of Energy
under Contract No. DE-AC02-83CH10093

Prepared under Task No. PV110604

October 1992

NOTICE

Printed in the United States of America
Available from:
National Technical Information Service
U.S. Department of Commerce
5285 Port Royal Road
Springfield, VA 22161

Price: Microfiche A01
Printed Copy A03

Codes are used for pricing all publications. The code is determined by the number of pages in the publication. Information pertaining to the pricing codes can be found in the current issue of the following publications which are generally available in most libraries: *Energy Research Abstracts (ERA)*; *Government Reports Announcements and Index (GRA and I)*; *Scientific and Technical Abstract Reports (STAR)*; and publication NTIS-PR-360 available from NTIS at the above address.

Printed on recycled paper

PREFACE

This report gives a summary of the fiscal year 1991 research activities and results under the Solar Radiation Research Task of the Photovoltaic Advanced Research and Development Project at the National Renewable Energy Laboratory (NREL).

TABLE OF CONTENTS

LIST OF FIGURES

LIST OF TABLES

1.0 INTRODUCTION

NREL's Photovoltaic (PV) Solar Radiation Research Task directly supports the characterization, testing, and design of PV cells, modules, and systems. The development of a scientific and engineering understanding of incident (i.e., available to PV devices) solar irradiance and the appropriate instrumentation systems and measurement methods are the activities and results of this project.

Previous results have been reported (selected examples) [1-8] in the literature. In this report we summarize more recent activities and results. The major recent activities have consisted of the completion of the Atmospheric Optical Calibration System (AOCS) and the comparison of instrumentation systems that collect site-specific measurements of solar irradiance for the purpose of PV system feasibility studies and/or design.

2.0 ATMOSPHERIC OPTICAL CALIBRATION SYSTEM

It is well known that atmospheric optical parameters and the spectral solar irradiance incident on a PV device are significant determinants of that device's performance characteristics (e.g., short-circuit current, efficiency, and power output). When testing PV devices outdoors, the incident spectral solar irradiance conditions are quite variable and are determined by extraterrestrial solar irradiance characteristics, the optical transmittance properties of the intervening atmosphere, the slant path of the direct-beam sunlight through the atmosphere (i.e., relative air mass), and the reflectance properties of the ground as viewed by the PV device.

Each type of PV device has a certain spectral response, so that its performance (e.g., efficiency, power output) depends on the solar spectral irradiance $E(\lambda)$ incident on the PV device [8]. Several methods are used to account for this spectral dependence. These include the use of reference PV cells and corrections of the PV data to simultaneously measured $E(\lambda)$ data [9]. The reference-cell method has a shortcoming consisting of a need to have spectral matching between the reference cell and the test device. Special techniques and specially configured solar spectroradiometers are required to accurately measure $E(\lambda)$. The shortcomings of this approach are a lack of suitable spectroradiometers, high costs, and voluminous data reduction.

The AOCS (U.S. Patent No. 4,779,980) is a multichannel solar radiometer system [7] developed to perform real-time measurements of the optical transmittance properties of the atmosphere at selected wavelengths within the solar spectral region (0.3 to 3.0 μm). These measurements include aerosol turbidity at 0.368, 0.500, and 0.862 μm, diffuse-horizontal to global-horizontal photon-flux ratio, and precipitable water vapor. An AOCS engineering report and user's manual is being prepared.

The AOCS consists of four narrow-band and six broad-band optical channels and two ancillary channels; the optical channels are listed in Table 2-1. All of the optical channels use silicon detectors. Channels 1-4 have 0.010-μm bandwidth (full width at half-maximum) filters; channels 6, 8, and 10 are filtered to produce a signal proportional to the total quantum flux from 0.4 to 0.7 μm; and channels 5, 7, and 9 are unfiltered. All direct-normal channels, the instrument temperature sensor (channel 11), and a data acquisition microcomputer are housed in a hermetically sealed, direct-beam module, shown in Figure 2-1. The data acquisition and downloading sequence is initiated, via the RS-232C serial port, on command from a host computer; this computer is also used to process, plot, print, and store the data. Data are generally taken every 5 minutes.

The ancillary channels measure instrument temperature (for correcting the optical data to reference temperature conditions) and atmospheric pressure (used in the precipitable water vapor calculations).

The four narrow-band optical channels (1-4) were calibrated using the Langley plot method [10]. Measurements were made every 5 minutes on six predominantly cloud-free days. To determine the calibration, a straight-line fit of the natural log of signal vs. relative air mass (M) was

extrapolated to the air-mass-zero intercept value (ln [Vo]) for each channel. A major shortcoming of the Langley plot method is that data depart from linearity due to changes throughout the day in atmospheric aerosol, water vapor, and clouds in the vertical equivalent direct solar path. Our results show that a considerable reduction in uncertainty in ln (Vo) can be obtained using statistical analysis. Two techniques were used sequentially: (1) the removal of selected outliers using the modified Thompson-Tau Technique and (2) the use of weighted averages. These methods are described in the literature [11,12].

Subsequent to Thompson-Tau analysis, a weighted average ln (Vo) for all runs was calculated. Weighting functions proportional to the reciprocal of the square of the standard deviation on the data for each day were used; thus data with low values of standard deviation were weighted significantly more than those with higher standard deviations. Results before and after statistical analysis are shown in Table 2-2.

Table 2-1. AOCS Optical Channels

Channel No.	Wavelength (μm)	Field of View (degrees)	Used to Calculate
Direct Normal			
1	0.368	2.3	Aerosol optical depth
2	0.500	2.3	Aerosol optical depth
3	0.862	2.3	Aerosol optical depth and precipitable water vapor
4	0.942	2.3	Precipitable water vapor
5	0.3-1.1	5.7	Total direct-normal irradiance
6	0.4-0.7	5.7	Total direct-normal quantum flux
Global Horizontal			
7	0.3-1.1	180	With channel 5, total global horizontal diffuse irradiance
8	0.4-0.7	180	With channel 6, ratio of diffuse skylight photon flux density to global-horizontal photon flux density
Tilt Surface			
9	0.3-1.1	180	Global irradiance in tilt plane
10	0.4-0.7	0	Photon flux in tilt plane

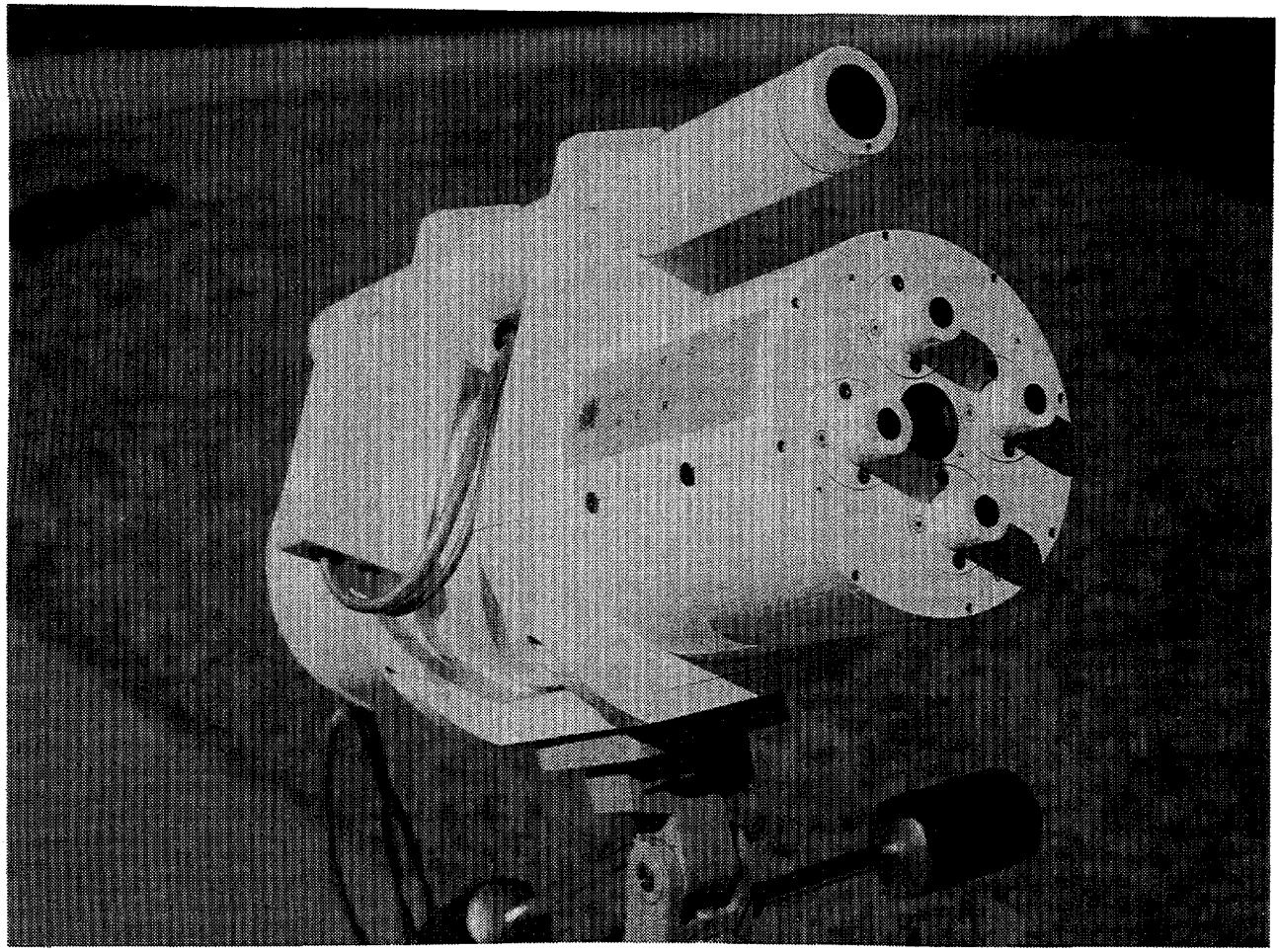

Figure 2-1. AOCS direct-beam module. The smaller tube is the direct-normal photon-flux channel.

Table 2-2. Comparison of Calibration Value ln (Vo) for the AOCS 0.500-μm Channel from Six Predominantly Clear-Sky Cases, With and Without Statistical Analysis

Value	Before Statistical Analysis	After Statistical Analysis
Average	6.717	6.868
Weighted average	N/A	6.870
Precision index (PI)	0.274	0.00125
Percent PI	4.08	0.0182
Number of data points	589	399

Note the significant reduction in the percent precision index (standard deviation ÷ ave. x 100) by the elimination of 190 outliers (0.018% vs. 4.08%). Similar results were obtained for all four narrow-band channels. There is no indication of monotonic temporal drift over the 13-month data acquisition period.

The broad-band optical channels (5-10) were calibrated outdoors against reference instruments [7]. The quantum sensors (8 and 10) were calibrated against a National Institute of Standards and Technology (NIST) spectral-irradiance lamp standard in the NREL optics laboratory. The temperature and atmospheric pressure channels (11 and 12, respectively) were calibrated by the NREL metrology laboratory against reference instruments. Calibration data for both narrow- and broad-band channels were corrected for the temperature of the instrument.

An equation for precipitable water vapor (PWV) as a function of atmospheric optical transmission can be derived from the fundamental equations of optical transmission found in Leckner [13] and other sources,

$$W_v = \frac{1}{M}\,\frac{1}{K5}\,\left(\frac{p}{p_o}\right)^k \left[\ln\left(K3\,\frac{V862}{V942}\right)\right]^{N3} \qquad (1)$$

where

W_v = the PWV in cm in the vertical direction
M = relative air mass
K5 = units constant
p = station pressure in kPa
p_o = 101.3 kPa
V862 = AOCS signal in water-vapor window at 0.862 μm
V942 = AOCS signal in water-vapor absorption band at 0.942 μm
K3 = the ratio V942/V862 under exoatmospheric conditions (i.e., Vo942/Vo862)
N3 = power-law dependence coefficient
k = pressure dependency exponent.

If a model with exponential decay of the atmospheric pressure, water vapor density, and pressure-temperature correction with height above reference are assumed, then it can be shown that K5 = 0.44, k = -2.54, and N3 = 1.8.

In order to more realistically determine these constants and their uncertainties for Denver, Colorado, all of the 1989 sounding data from the National Weather Service facility at Stapleton International Airport were used to calculate W_v using direct integration of water vapor; the corresponding values of atmospheric transmission at 0.862 and 0.942 μm were calculated directly. By writing Eq. 1 in the form

$$y = a_o + a_1 x_1 + a_2 x_2 \qquad (2)$$

where

$y = \ln (M \times W_v)$
$a_o = -\ln K5$
$a_1 = k$
$a_2 = N3$
$x_1 = \ln (p/p_o)$
$x_2 = \ln [-\ln \tau_{w942}]$
$\tau_{w942} = V942/Vo942$

assuming V862/Vo862 = 1 in the optical window, we can solve the matrix equation

$$Y = A X \tag{3}$$

where Y represents the integrated PWV data from the soundings, A the coefficient matrix, and X the calculated values x_1 and x_2. The method of LU-Decomposition and back substitutions, together with an error estimation routine, were written to solve this equation for A (i.e., a_o, a_1, and a_2). The final values are shown in Table 2-3, along with the original values and the values from the model.

The K3 values are dependent on both the detector sensitivies and filter transmission factors for the two channels; one would not expect the value for the model to be the same as for the instrument. It is gratifying that the other two K3 values agree so well since they are derived using quite different methods. The value of k is sensitive to the vertical pressure profile; the difference in values shown is probably due to departure of the actual profiles from the exponential form used for the model.

Table 2-3. Constants for the Precipitable Water Vapor Equation Determined by Various Methods

Constant	Model	Original Value	New Value
K3	0.807[a]	0.506[b]	0.545[c]
K5	0.44	0.254[b]	0.25[d]
k	-2.54	-0.960[b]	-1.19[d]
N3	1.8	1.82[b]	1.9[d]

[a]Based on the measured ratio of the extraterrestrial spectral irradiance value at 0.942 μm to that at 0.862 μm.
[b]Based on optical transfer of a three-site sunphotometer calibration against microwave radiometers.
[c]From the AOCS Langley plots at 0.862 and 0.942 μm.
[d]From the Stapleton sounding analysis.

Figure 2-2 shows a plot of aerosol-scattering turbidity at 0.500 μm (τ_{500}) times M vs. the horizontal plane global-diffuse-to-total-global photon-flux ratio (SHGH). The heavy line represents the functional relationship calculated using a model for absolute air mass values from 1.25 to 4.00 and for the normally expected range of τ_{500} values. The box indicates American Society for Testing and Materials (ASTM) standard conditions [14]. The points on this plot are calculated from measurements made on 15 October 1987, which indicate foggy (run 140), clear (runs 141-151), and various cloudy conditions (runs 152-157). Note that under clear-sky conditions the data lie close to reference conditions while under the influence of fog and clouds, the data lie away from reference conditions because of the influence of light scattering by the clouds and fog. None of the data taken during this run met ASTM standard conditions. The lines parallel to the reference line indicate boundaries of the region within which spectral mismatch corrections [9] may be possible. The exact location of the boundary lines and the size of the ASTM standard condition box are continuing subjects of research for our task.

Figure 2-3 shows normalized efficiency for an amorphous PV device plotted against the AOCS parameter Δ , which is defined as

$$\Delta = \sqrt{\sum_{i=1}^{3} \delta_i^2} \qquad (4)$$

where

$\delta_1 = SHGH_{meas} - SHGH_{ref}$
$\delta_2 = (\tau_{500} \times M)_{meas} - (\tau_{500} \times M)_{ref}$
$\delta_3 = PWV_{meas} - PWV_{ref}$.

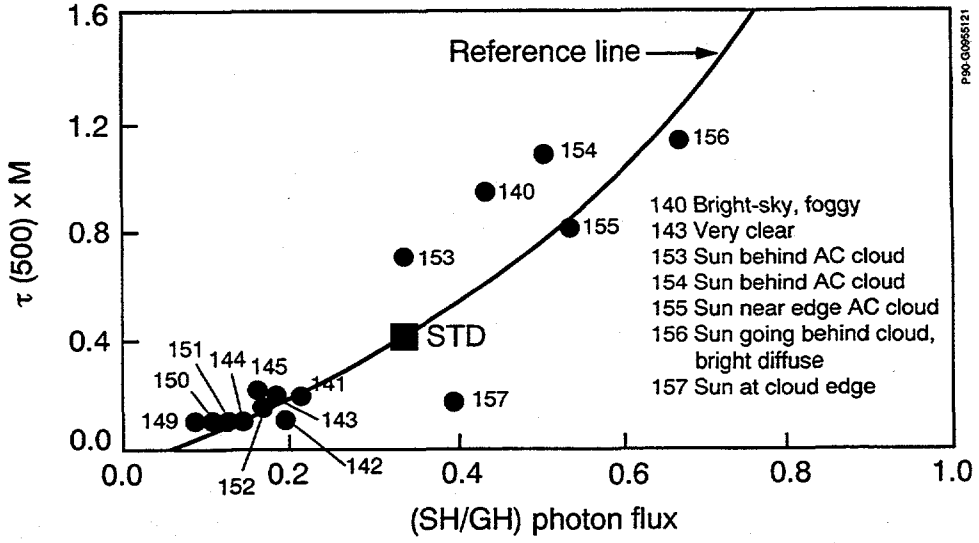

Figure 2-2. Modeled and measured aerosol-scattering turbidity at 0.500 μm x M vs. the diffuse-horizontal to global-horizontal photon-flux ratio

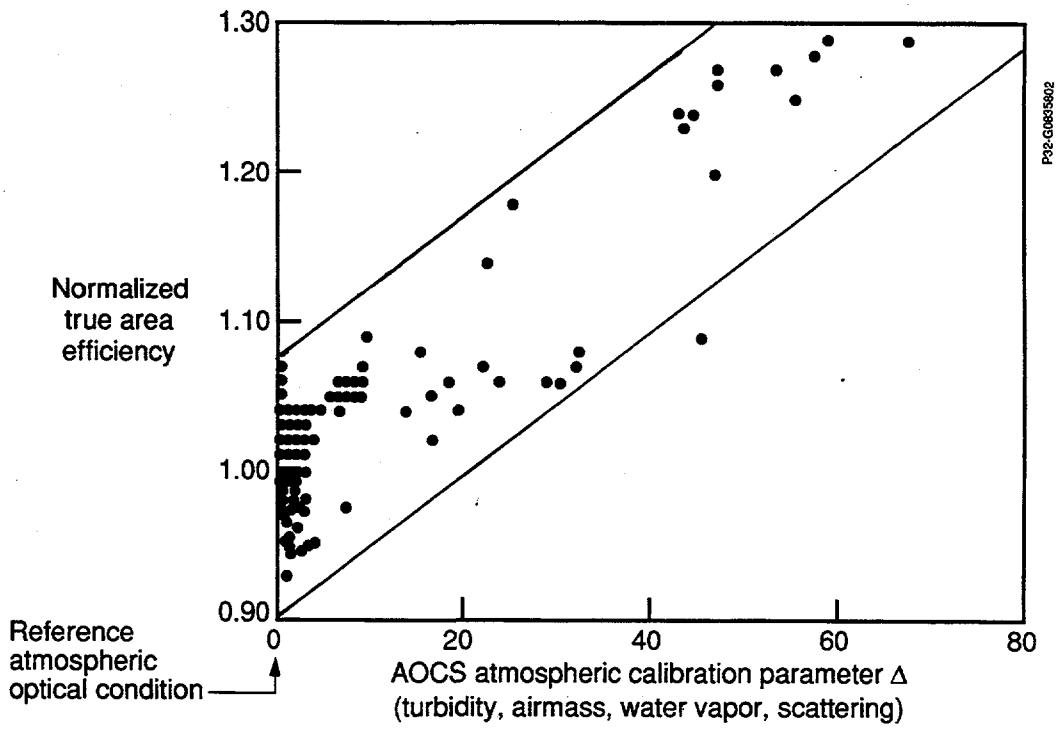

Figure 2-3. Relationship between the efficiency and the atmospheric parameters measured by the AOCS for an amorphous silicon PV module

Because efficiency under clear-sky conditions is a function of M, the measured efficiency values under all sky conditions were normalized to a least-squares fit of clear-sky efficiency vs. M. Figure 2-3 clearly indicates a relationship between the efficiency and the atmospheric parameters measured by the AOCS; almost all of the data lie between the two parallel lines. Test data for a PV device can be weighted or rejected depending on the AOCS-derived value of Δ at the time each measurement is made. This represents a specific application of the AOCS for outdoor PV device testing.

The vertical distance between the parallel lines represents uncertainty in the data that are not accounted for by Δ. This uncertainty can be a combination of random errors in the PV device or AOCS measurements, as well as dependence on atmospheric parameters that are not included in the analysis.

We have shown that atmospheric conditions that determine $E(\lambda)$ can be monitored with the AOCS while taking PV device data, enabling researchers to observe correlations between efficiency and other PV parameters and $E(\lambda)$ variations.

We have also shown the utility of the AOCS to outdoor PV device testing. The AOCS will continue to be used to support NREL's outdoor testing of PV devices. We expect to advance the outdoor testing and understanding of PV device performance and reliability by using the AOCS to delineate and account for "atmospheric effects."

3.0 SOLAR IRRADIANCE MEASUREMENT SYSTEMS

The Electric Power Research Institute (EPRI) and NREL are currently conducting a joint project [6] to compare the field performance of several types of solar irradiance measurement systems available to electric utilities [15] for determining global, diffuse, and direct solar irradiance availability in their service territories.

The solar irradiance measurement instruments include pyranometers for measuring global-horizontal and plane-of-array irradiance, and pyrheliometers with solar trackers for measuring direct-normal irradiance. These are the more conventional options for obtaining global-horizontal, plane-of-array, and direct irradiance, such as measuring global-horizontal irradiance using a pyranometer and measuring diffuse-horizontal irradiance using a pyranometer with an adjustable shadowband. Then the direct and plane-of-array irradiance are calculated from the global and diffuse measurements, the sun's zenith angle, and the orientation of the array.

Rotating shadowband radiometers (RSRs) provide another option for determining global, direct, and diffuse irradiance using a single unit from which PV plane-of-array irradiance can be calculated. Two manufacturers (Ascension Technology Inc., ATI, and the State University of New York at Albany, SUNYA) have developed RSRs. An instrument from each of the two manufacturers was purchased and integrated into NREL's baseline solar radiation measurement system at the Solar Radiation Research Laboratory (SRRL) on South Table Mountain in Golden, Colorado, for a 6-month test period.

The RSRs use a commercially available silicon-detector pyranometer to measure global-horizontal irradiance and to measure diffuse irradiance when the rotating shadowband blocks the direct beam during the band's rotation; direct irradiance is calculated from the total and diffuse measurements and the sun's zenith angle (global horizontal = diffuse horizontal + direct normal x cosine of zenith angle). Differences between the two RSRs include sampling scheme and associated algorithms and treatment of the diffuse irradiance measurements.

From early January through early July 1991, NREL [6] acquired 1-minute data from the two RSRs as well as 5-minute data from the NREL instrumentation: a pyranometer (measuring global-horizontal solar radiation), a pyrheliometer mounted in a solar tracker (measuring direct-normal solar radiation), and a pyranometer with a shadowband (measuring diffuse-horizontal solar radiation).

Our preliminary comparisons (among our SRRL instruments and the RSRs) show that the daily direct, global, and diffuse totals have coefficients of determination (square of the correlation coefficient) of greater than 0.98 and root mean square differences of 2.5% to 4.4%, except for the comparison of NREL (SRRL) and ATI diffuse (11.7%). Further analyses will be performed such as comparing all systems (SRRL, SUNYA, and ATI) with the NREL reference cavity radiometer and tracking disk system, which provides the most accurate reference irradiances. A rigorous comparison of final results will be based on the final measurement uncertainty analyses utilizing data acquired from the experiment and a final post-experiment uncertainty analysis.

Full 6-month results and statistics for 5-minute averages and hourly and daily totals are being compiled for a final test report, which will be available from EPRI and NREL.

Our preliminary evaluation [6] indicates that all instruments (including the RSRs) in the comparison can be considered as options for measuring solar irradiance and monitoring for resource assessment. However, we must recognize that the RSRs are still under development, and there is limited field experience to date.

4.0 REFERENCES

1. R.L. Hulstrom, R.E. Bird, and C.J. Riordan, *Solar Cells*, 15, (1985) 365.

2. R.E. Bird and C.J. Riordan, *Journal of Climate and Applied Metrology*, Vol. 25, No. 1, (1986), p. 87.

3. C.J. Riordan, *Solar Cells*, 18, (1988), 223.

4. R.L. Hulstrom and T.W. Cannon, *Solar Cells*, 21, (1987), 329.

5. T.W. Cannon and R.L. Hulstrom, SPIE, 1109, (1989), 152.

6. T. Stoffel, C.J. Riordan, and J. Bigger, *Proceedings of the Twenty-Second IEEE Photovoltaics Specialists Conference 1991*, Vol. 1, (1991), 533.

7. T.W. Cannon, SPIE (Proceedings of the 14th Symposium on Photonic Measurements), (1992), 1712.

8. P. Faine, S.R. Kurtz, C.J. Riordan, and J.M. Olson, *Solar Cells*, 31, (1991), 259.

9. C.R. Osterwald, K.A. Emery, D.R. Myers, and R.E. Hart, *Proceedings of IEEE Photovoltaic Specialists Conference*, Vol. II, (1990), 1062.

10. G.E. Shaw, J.A. Reagan, and B.M. Herman, *J. Appl. Meteorol.*, Vol. 12, (1973), 374.

11. R. Abernathy and R. Benedict, *ISA Trans.*, Vol. 24, (1985), 74.

12. ASME Standard PTC 19.1-1985, New York: American Society of Mechanical Engineers, (1985).

13. B. Leckner, *Solar Energy*, Vol. 20, (1978), 143.

14. 1987 Annual Book of ASTM Standards, Nuclear, Solar and Geothermal Energy, Vol. 12.02, (1987), 673.

15. V. Risser, S. Durand, and D. Bowling, Interim Report GS-7082, Palo Alto, CA: Electric Power Research Institute, (1990).

Document Control Page	1. NREL Report No. NREL/TP-411-5013	2. NTIS Accession No. DE92016430	3. Recipient's Accession No.
4. Title and Subtitle Photovoltaic Advanced Research and Development Project: Solar Radiation Research Annual Report			5. Publication Date October 1992 6.
7. Author(s) R. Hulstrom, T. Cannon, T. Stoffel, and C. Riordan			8. Performing Organization Rept. No.
9. Performing Organization Name and Address National Renewable Energy Laboratory 1617 Cole Blvd. Golden, CO 80401			10. Project/Task/Work Unit No. PV110604 11. Contract (C) or Grant (G) No. (C) (G)
12. Sponsoring Organization Name and Address National Renewable Energy Laboratory 1617 Cole Blvd. Golden, CO 80401-3393			13. Type of Report & Period Covered Technical Report 1 October 1990 - 30 September 1991 14.

15. Supplementary Notes
NREL technical monitor:

16. Abstract (Limit: 200 words)

This report is a summary of the fiscal year 1991 research activities and results under the Solar Radiation Research task of the Photovoltaic (PV) Advanced Research and Development project at the National Renewable Energy Laboratory (NREL). This task directly supports the characterization, testing, and design of PV cells, modules, and systems. The development of a scientific and engineering understanding of incident (i.e., available to PV devices) solar irradiance and the appropriate instrumentation systems and measurement methods are the activities and results of this project. Activities described in this report include the completion of the Atmospheric Optical Calibration Systems (AOCS) and the comparison of instrumentation systems that collect site-specific measurements of solar irradiance for the purpose of PV system feasibility studies and/or design.

17. Document Analysis
a. Descriptors
solar radiation ; photovoltaics ; solar cells

b. Identifiers/Open-Ended Terms

c. UC Categories
270, 233

18. Availability Statement	19. No. of Pages
National Technical Information Service U.S. Department of Commerce 5285 Port Royal Road Springfield, VA 22161	18 20. Price A03

Form No. 0069E (6-30-87)